

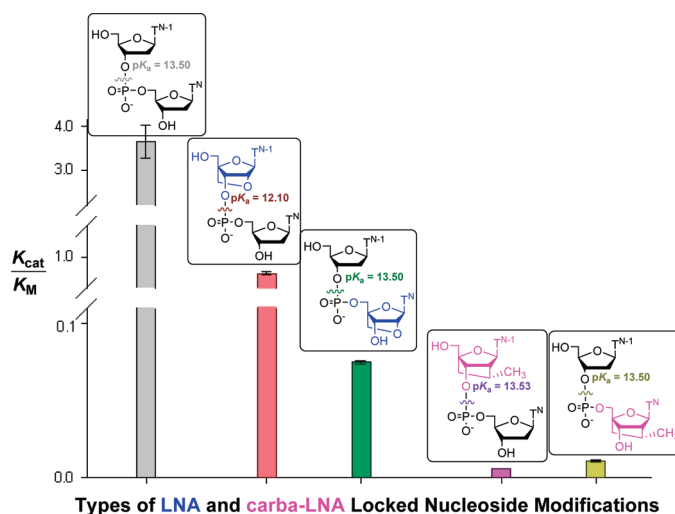
# Why Carba-LNA-Modified Oligonucleotides Show Considerably Improved 3'-Exonuclease Stability Compared to That of the LNA Modified or the Native Counterparts: A Michaelis–Menten Kinetic Analysis

Chuanzheng Zhou and Jyoti Chattopadhyaya\*

Bioorganic Chemistry Program, Department of Cell and Molecular Biology, Box 581, Biomedical Centre, Uppsala University, SE-751 23 Uppsala, Sweden

jyoti@boc.uu.se.

Received February 1, 2010



In this study, 12 different native or LNA, carba-LNA-modified dinucleoside phosphates were designed as simple chemical models to study how carba-LNA modifications improve the 3'-exonuclease (SVPDE in this study) resistance of internucleotidic phosphate compared to those exhibited by LNA-modified and the native counterparts. Michaelis–Menten kinetic studies for dimers **3**–**7**, in which the LNA or carba-LNA modifications are located at the 5'-end, showed that (i) increased 3'-exonuclease resistance of  $5'$ [LNA-T] $_p$ T (**3**) compared to the native  $5'$ T $_p$ T (**1**) was mainly attributed to steric hindrance imposed by the LNA modification that retards the nuclease binding ( $K_M$ ) and (ii) digestion of  $5'$ [carba-LNA-dT] $_p$ T (**4**) and  $5'$ [LNA-T] $_p$ T (**3**), however, exhibit similar  $K_M$ s, whereas the former shows a 100× decrease in  $K_{cat}$  and is hence more stable than the latter. By studying the correlation between  $\log k_{cat}$  and  $pK_a$  of the departing 3'(or 6')-OHs for **3**–**7**, we found the  $pK_a$  of 3'-OH of carba-LNA-T was 1.4  $pK_a$  units higher than that of LNA-T, and this relatively less acidic character of the 3'-OH in the former leads to the 100× decrease in the catalytic efficiency for the digestion of  $5'$ [carba-LNA-T] $_p$ T (**4**). In contrast, Michaelis–Menten kinetic studies for dimers **9**–**12**, with the LNA or carba-LNA modifications at the 3'-end, showed that the digestion of  $5'$ T $_p$ [LNA-T] (**9**) exhibited similar  $K_M$  but  $k_{cat}$  decreased around 40 times compared to that of the native  $5'$ T $_p$ T (**1**). Similar  $k_{cat}$  values have been observed for digestion of  $5'$ T $_p$ [carba-LNA-T] (**10**) and  $5'$ T $_p$ [LNA-T] (**9**). The higher stability of carba-LNA modified dimer **10** compared with LNA modified dimer **9** comes solely from the increased  $K_M$ .

## Introduction

The therapeutic potential of antisense oligonucleotides (AON)<sup>1,2</sup> and small interference RNA (siRNA)<sup>3,4</sup> has attracted considerable attention in recent years. One of the

most important criteria in this regard is that an oligonucleotide should be nuclease resistant in order to maximize its chances (in terms of its stability) of penetrating the cell and binding to the target RNA and be recognized in its duplex

form by the cleaving enzymes, RNase H<sup>5</sup> in the case of AON strategy and argonaute proteins in the case of RNAi.<sup>6</sup> Finding solutions to the problems in all of these steps is essential to modulate the pharmacokinetic and pharmacodynamic properties in order to devise successful therapeutics.

Chemical modification represents the most popular strategy to construct nuclease-resistant therapeutic AONs<sup>2,7</sup> and siRNAs.<sup>3,4,8</sup> There are many different types of modified nucleotides reported thus far in the literature;<sup>9–12</sup> in particular, in the past decade, locked nucleic acid (LNA)<sup>13</sup> and its derivatives<sup>14–20</sup> have attracted considerable interest.<sup>21</sup> LNA exhibits unprecedented affinity ( $\Delta T_m = 3–8$  °C per modification depending upon the sequence context) toward complementary DNA and RNA, which endows it with broad application in biotechnology and therapeutics.<sup>22</sup> Although it was reported that LNA-modified AON and siRNA showed improved nuclease resistance and functionality,<sup>23–25</sup> this improvement on nuclease resistance is, however, minimal compared to

that of the native counterpart.<sup>26</sup> Hence, consecutive LNA modifications<sup>27</sup> in combination with the phosphorothiate linkage<sup>28</sup> have been used for therapeutic application of LNA-modified oligonucleotides. Recently, our group has reported the synthesis of several derivatives of carba-LNA nucleoside through a radical cyclization approach.<sup>29–33</sup> The structural difference between LNA nucleoside and carba-LNA nucleoside lies in the fact that the 2'-O- in LNA is replaced with –CHR– functionality in carba-LNA (in which R can be either a carbon<sup>29</sup> or a heteroatom<sup>31</sup>). Our radical cyclization approach also opened unique possibilities to functionalize the other carbon atom (i.e., at C6') in the fused carba-ring with other substituents.<sup>29–31</sup> This fine-tuning does not result in major structure variations in terms of recognition of the complementary DNA or RNA strand, but carba-LNA nucleoside modified oligonucleotides showed considerably improved nuclease resistance relative to LNA nucleoside modified counterparts. In the present study, several dinucleoside monophosphates modified with LNA or carba-LNA nucleoside derivatives were used as the chemical models to answer the question of why carba-LNA modification is much better than LNA modification in the engineering of the nuclease resistance to the oligonucleotides. Clearly, answers to this question may in the future allow us to design improved nucleotides for putative therapeutic applications.

It was known that the metabolism of oligonucleotides in vivo involves degradation by both exo- and endonucleases, whereas the predominant nuclease activity comes from a 3'-exonuclease<sup>34</sup> such as phosphodiesterase I (EC 3.1.4.1).<sup>35</sup> Phosphodiesterase I from *Crotalus adamanteus* (also known as snake venom phosphodiesterase, SVPDE) is the most popular 3'-exonuclease used for testing the nuclease resistance of modified AONs.<sup>11,12,15,16,26,36–39</sup> In this study, kinetic studies of digestion of chemical models by SVPDE, together with the comparison of the pK<sub>a</sub>'s of the departing 3'-OHs during SVPDE digestion, suggested that both steric and electrostatic effects contribute to the improved 3'-exonuclease resistance for LNA- and especially carba-LNA-modified oligonucleotides.

(1) Bennett, C. F.; Swayze, E. E. *Annu. Rev. Pharmacol. Toxicol.* **2010**, *50*, 259–293.

(2) Croke, S. T. *Annu. Rev. Med.* **2004**, *55*, 61–95.

(3) Bumcrot, D.; Manoharan, M.; Koteliansky, V.; Sah, D. W. Y. *Nature Chem. Biol.* **2006**, *2*, 711–719.

(4) Watts, J. K.; Deleavey, G. F.; Damha, M. J. *Drug Discov. Today* **2008**, *13*, 842–855.

(5) Nowotny, M.; Gaidamakov, S. A.; Crouch, R. J.; Yang, W. *Cell* **2005**, *121*, 1005–1016.

(6) Tolia, N. H.; Joshua-Tor, L. *Nature Chem. Biol.* **2007**, *3*, 36–43.

(7) Uhlmann, E.; Peyman, A. *Chem. Rev.* **1990**, *90*, 543–584.

(8) Bramsen, J. B.; Laursen, M. B.; Nielsen, A. F.; Hansen, T. B.; Bus, C.; Langkjaer, N.; Babu, B. R.; Hojland, T.; Abramov, M.; Van Aerschot, A.; Odadzic, D.; Smicius, R.; Haas, J.; Andree, C.; Barman, J.; Wenska, M.; Srivastava, P.; Zhou, C. Z.; Honcharenko, D.; Hess, S.; Muller, E.; Bobkov, G. V.; Mikhailov, S. N.; Fava, E.; Meyer, T. F.; Chattopadhyaya, J.; Zerial, M.; Engels, J. W.; Herdewijn, P.; Wengel, J.; Kjems, J. *Nucleic Acids Res.* **2009**, *37*, 2867–2881.

(9) Manoharan, M. *Biochem. Biophys. Acta* **1999**, *1489*, 117–130.

(10) Egli, M.; Minasov, G.; Tereshko, V.; Pallan, P. S.; Teplova, M.; Inamati, G. B.; Lesnik, E. A.; Owens, S. R.; Ross, B. S.; Prakash, T. P.; Manoharan, M. *Biochemistry* **2005**, *44*, 9045–9057.

(11) Teplova, M.; Wallace, S. T.; Tereshko, V.; Minasov, G.; Symons, A. M.; Cook, P. D.; Manoharan, M.; Egli, M. *Proc. Natl. Acad. Sci. U.S.A.* **1999**, *96*, 14240–14245.

(12) Maier, M. A.; Leeds, J. M.; Balow, G.; Springer, R. H.; Bharadwaj, R.; Manoharan, M. *Biochemistry* **2002**, *41*, 1323–1327.

(13) Singh, S. K.; Nielsen, P.; Koshkin, A. A.; Wengel, J. *Chem. Commun.* **1998**, 455–456.

(14) Morita, K.; Hasegawa, C.; Kaneko, M.; Tsutsumi, S.; Sone, J.; Ishikawa, T.; Imanishi, T.; Koizumi, M. *Bioorg. Med. Chem. Lett.* **2002**, *12*, 73–76.

(15) Kuwahara, M.; Obika, S.; Takeshima, H.; Hagiwara, Y.; Nagashima, J.; Ozaki, H.; Sawai, H.; Imanishi, T. *Bioorg. Med. Chem. Lett.* **2009**, *19*, 2941–2943.

(16) Rahman, S. M. A.; Seki, S.; Obika, S.; Yoshikawa, H.; Miyashita, K.; Imanishi, T. *J. Am. Chem. Soc.* **2008**, *130*, 4886–4896.

(17) Honcharenko, D.; Barman, J.; Varghese, O. P.; Chattopadhyaya, J. *Biochemistry* **2007**, *46*, 5635–5646.

(18) Albaek, N.; Petersen, M.; Nielsen, P. *J. Org. Chem.* **2006**, *71*, 7731–7740.

(19) Enderlin, G.; Nielsen, P. *J. Org. Chem.* **2008**, *73*, 6891–6894.

(20) Seth, P. P.; Siwkowski, A.; Allerson, C. R.; Vasquez, G.; Lee, S.; Prakash, T. P.; Kinberger, G.; Migawa, M. T.; Gaus, H.; Bhat, B.; Swayze, E. E. *Nucleic Acids Symp. Ser.* **2008**, *52*, 553–554.

(21) Zhou, C.; Chattopadhyaya, C. *Curr. Opin. Drug Discov. Dev.* **2009**, *12*, 876–898.

(22) Kaur, H.; Babu, B. R.; Maiti, S. *Chem. Rev.* **2007**, *107*, 4672–4697.

(23) Wahlestedt, C.; Salmi, P.; Good, L.; Kela, J.; Johnsson, T.; Hokfelt, T.; Broberger, C.; Porreca, F.; Lai, J.; Ren, K. K.; Ossipov, M.; Koshkin, A.; Jakobsen, N.; Skouv, J.; Oerum, H.; Jacobsen, M. H.; Wengel, J. *Proc. Natl. Acad. Sci. U.S.A.* **2000**, *97*, 5633–5638.

(24) Elmen, J.; Thonberg, H.; Ljungberg, K.; Frieden, M.; Westergaard, M.; Xu, Y. H.; Wahren, B.; Liang, Z. C.; Urum, H.; Koch, T.; Wahlestedt, C. *Nucleic Acids Res.* **2005**, *33*, 439–447.

(25) Mook, O. R.; Baas, F.; de Wissel, M. B.; Fluiter, K. *Mol. Cancer Ther.* **2007**, *6*, 833–843.

(26) Morita, K.; Takagi, M.; Hasegawa, C.; Kaneko, M.; Tsutsumi, S.; Sone, J.; Ishikawa, T.; Imanishi, T.; Koizumi, M. *Bioorg. Med. Chem.* **2003**, *11*, 2211–2226.

(27) Frieden, M.; Hansen, H. F.; Koch, T. *Nucleosides Nucleotides Nucleic Acids* **2003**, *22*, 1041–1043.

(28) Kumar, R.; Singh, S. K.; Koshkin, A. A.; Rajwanshi, V. K.; Meldgaard, M.; Wengel, J. *Bioorg. Med. Chem. Lett.* **1998**, *8*, 2219–2222.

(29) Srivastava, P.; Barman, J.; Pathmasiri, W.; Plashkevych, O.; Wenska, M.; Chattopadhyaya, J. *J. Am. Chem. Soc.* **2007**, *129*, 8362–8379.

(30) Zhou, C.; Liu, Y.; Andaloussi, M.; Badgujar, N.; Plashkevych, O.; Chattopadhyaya, J. *J. Org. Chem.* **2009**, *74*, 118–134.

(31) Xu, J. F.; Liu, Y.; Dupouy, C.; Chattopadhyaya, J. *J. Org. Chem.* **2009**, *74*, 6534–6554.

(32) Zhou, C. Z.; Plashkevych, O.; Chattopadhyaya, J. *Org. Biomol. Chem.* **2008**, *6*, 4627–4633.

(33) Zhou, C. Z.; Plashkevych, O.; Liu, Y.; Badgujar, N.; Chattopadhyaya, J. *Heterocycles* **2009**, *78*, 1715–1728.

(34) Shaw, J. P.; Kent, K.; Bird, J.; Fishback, J.; Froehler, B. *Nucleic Acids Res.* **1991**, *19*, 747–750.

(35) Hynie, I.; Meuffels, M.; Poznanski, W. *J. Clin. Chem.* **1975**, *21*, 1383–1387.

(36) Prhavc, M.; Prakash, T. P.; Minasov, G.; Cook, P. D.; Egli, M.; Manoharan, M. *Org. Lett.* **2003**, *5*, 2017–2020.

(37) Cummins, L. L.; Owens, S. R.; Risen, L. M.; Lesnik, E. A.; Freier, S. M.; McGee, D.; Guinasso, C. J.; Cook, P. D. *Nucleic Acids Res.* **1995**, *23*, 2019–2024.

(38) Miyashita, K.; Rahman, S. M. A.; Seki, S.; Obika, S.; Imanishi, T. *Chem. Commun.* **2007**, 3765–3767.

(39) Damha, M. J.; Giannaris, P. A.; Marfey, P. *Biochemistry* **1994**, *33*, 7877–7885.

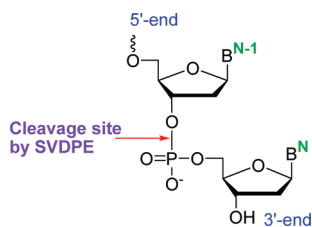


**FIGURE 1.** Cleavage of 3′O–P bond at the 3′-end nucleotide by 3′-exonuclease, SVPDE.

## Results and Discussion

**1.0. Design and Synthesis of the Dimeric Model Systems 1–12.** It is known that 3′-exonuclease SVPDE-mediated phosphate scission involves recognition of the 3′-end nucleotide (number “N” in N-mer oligonucleotides, Figure 1) followed by the attack by threonine residue of the enzyme on the phosphate in line with the 3′-O of N<sup>−1</sup> nucleoside, which subsequently departs.<sup>40,41</sup> SVPDE can recognize a broad range of substrates including longer or shorter, native and/or modified nucleotides.<sup>42</sup> Dinucleoside monophosphates have only one internucleotidic phosphodiester linkage and are therefore convenient models for investigating the effect imposed by modification at either the “N” or “N<sup>−1</sup>” position<sup>43</sup> by Michaelis–Menten kinetics. In this study, we designed 12 dinucleoside monophosphates, and their structures are shown in Figure 2. T<sub>p</sub>T (1), U<sub>p</sub>T (2), and T<sub>p</sub>U (8) are native dimer nucleotides, whereas in the modified dimer nucleotides 3–7, the “N” nucleoside (3′-end) is thymidine (T) and the modified nucleosides at position “N<sup>−1</sup>” (5′-end) include LNA-T, carba-LNA-T, 6′(R)-OH-carba-LNA-T, and 6′(S)-OH-carba-LNA-T. These modified models were designed to study how the LNA-T or carba-LNA-T modifications at the “N<sup>−1</sup>” position can affect nuclease resistance of the internucleotidic phosphate. However, in dimers 9–12 the modifications located at position “N” (3′-end) provide simple models to study the effect of modifications at the “N” position.

These chemical models have been synthesized according to our previously published procedures,<sup>29,30,44</sup> and a brief description of the synthesis is presented in the Experimental Section.

**2.0. 3′-Exonuclease Resistance of the Internucleotidic Phosphate with 5′-End-Modified Dimers 3–7.** **2.1. Comparison of Relative Nuclease Resistance of 5′-Modified Dimers 3–7 with Native 1 and 2.** To compare the relative nuclease resistance of the internucleotidic phosphate with LNA-T or carba-LNA-T modifications at the “N<sup>−1</sup>” position, compounds 1–7 were treated with SVPDE under identical conditions (1 o.d. dimer, 100 mM Tris-HCl, pH 8.0, 100 mM NaCl, 15 mM MgCl<sub>2</sub>, SVPDE 30 μg/mL, 21 °C, total reaction volume 1 mL). Aliquots were taken at appropriate time points and analyzed by RP-HPLC (HPLC profiles are shown in Figure S1–11, Supporting Information). From the digestion curves shown in Figure 3A, we can see that the nuclease resistance

(*t*<sub>1/2</sub> of digestion) of dimers 1–7 decreases in the following order: <sup>5</sup>[carba-LNA-T]<sub>p</sub>T (4) (693 min) ≈ <sup>5</sup>[6′(S)-OH-carba-LNA-T]<sub>p</sub>T (6) (693 min) > <sup>5</sup>[3′-OH-carba-LNA-T]-6′<sub>p</sub>3′-T (7) (90 min) > <sup>5</sup>[6′(R)-OH-carba-LNA-T]<sub>p</sub>T (5) (15.3 min) > <sup>5</sup>[LNA-T]<sub>p</sub>T (3) (9.4 min) > <sup>5</sup>T<sub>p</sub>T (1) (1.9 min) ≈ <sup>5</sup>U<sub>p</sub>T (2) (1.2 min). Briefly, native dimers <sup>5</sup>T<sub>p</sub>T (1) and <sup>5</sup>U<sub>p</sub>T (2) were degraded by SVPDE very fast. LNA modification, as in <sup>5</sup>[LNA-T]<sub>p</sub>T (3), leads to slightly improved nuclease resistance, whereas <sup>5</sup>[carba-LNA-T]<sub>p</sub>T (4) was found to be nearly 100 times more stable than <sup>5</sup>[LNA-T]<sub>p</sub>T (3). Interestingly, nuclease resistance of the internucleotidic phosphate can be modulated significantly by addition of one C6′-OH to the “N<sup>−1</sup>” residue of carba-LNA-T modification. If the C6′-OH is oriented away from the internucleotidic phosphate, as in <sup>5</sup>[6′(S)-OH-carba-LNA-T]<sub>p</sub>dT (6), it does not lead to any significant effect on the stability of the phosphate. However, if the C6′-OH is directed toward the internucleotidic phosphate, as in <sup>5</sup>[6′(R)-OH-carba-LNA-T]<sub>p</sub>T (5), it immensely destabilizes the phosphate. The <sup>5</sup>[3′-OH-carba-LNA-T]-6′<sub>p</sub>5′-T (7) with the 6′→5′ phosphate linkage was also a good substrate for SVPDE. Its stability was found to be in between <sup>5</sup>[6′(R)-OH-carba-LNA-T]<sub>p</sub>T (5) and <sup>5</sup>[6′(S)-OH-carba-LNA-T]<sub>p</sub>dT (6).

**2.2. Comparison of Michaelis–Menten Kinetics of Digestion of 5′-Modified Dimers 3–7 with Those of Native Dimers 1 and 2.** To explore why different 5′-end modifications on “N<sup>−1</sup>” nucleosides in 3–7 result in such different impacts on the nuclease resistance of the internucleotidic phosphates, Michaelis–Menten kinetics<sup>45</sup> of digestion of these dimers by SVPDE have been carried out. Kinetic parameters were subsequently compared with those of the native dinucleoside phosphates 1 and 2 (Table 1).

**2.2.1. Different K<sub>M</sub> Modulations by Different 5′-End Modified Dimers.** The Michaelis constant (*K<sub>M</sub>*) of digestion of 1–7 decreases in the following order: <sup>5</sup>[6′(R)-OH-carba-LNA-T]<sub>p</sub>T (5) (545 μM) > <sup>5</sup>[carba-LNA-T]<sub>p</sub>T (4) (412 μM) ≈ <sup>5</sup>[LNA-T]<sub>p</sub>T (3) (365 μM) > <sup>5</sup>[6′(S)-OH-carba-LNA-T]<sub>p</sub>T (6) (250 μM) > <sup>5</sup>[3′-OH-carba-LNA-T]-6′<sub>p</sub>5′-T (7) (83 μM) > <sup>5</sup>T<sub>p</sub>T (1) (46 μM) > <sup>5</sup>U<sub>p</sub>T (2) (15 μM). Hence, <sup>5</sup>[LNA-T]<sub>p</sub>T (3) is bound by SVPDE about 10 times weaker than those of the native compounds. On the other hand, <sup>5</sup>[carba-LNA-T]<sub>p</sub>T (4) exhibits *K<sub>M</sub>* comparable to that of <sup>5</sup>[LNA-T]<sub>p</sub>T (3), so binding by nuclease is not the key factor that leads to the improved nuclease resistance for the former than for the latter. It is likely that a 6′-OH substituent in carba-LNA-T (“N<sup>−1</sup>”), as in <sup>5</sup>[6′(R)-OH-carba-LNA-T]<sub>p</sub>dT (5) and <sup>5</sup>[6′(S)-OH-carba-LNA-T]<sub>p</sub>dT (6), can slightly modulate the binding of SVPDE, compared to that of <sup>5</sup>[carba-LNA-T]<sub>p</sub>T (4), since their *K<sub>M</sub>*s are more or less comparable. An interesting observation is that although the 5 and 7 have the same modified “N<sup>−1</sup>” nucleoside, their different phosphate linkage topologies result in very different binding affinities by SVPDE in that <sup>5</sup>[3′-OH-carba-LNA-T]-6′<sub>p</sub>5′-T (7), which has the 6′→5′-phosphate linkage, can be bound by SVPDE much more effectively than that of <sup>5</sup>[6′(R)-OH-carba-LNA-T]<sub>p</sub>T (5).

The 1–2 orders of magnitude decrease in the binding affinity, *K<sub>M</sub>*, for <sup>5</sup>[LNA-T]<sub>p</sub>T (3) compared to those of the

(40) Culp, J. S.; Butler, L. G. *Arch. Biochem. Biophys.* **1986**, *246*, 245–249.

(41) Cleland, W. W.; Hengge, A. C. *Chem. Rev.* **2006**, *106*, 3252–3278.

(42) Dolapchiev, L. B. *Int. J. Biol. Macromol.* **1980**, *2*, 7–12.

(43) Richards, G. M.; Tutas, D. J.; Wechter, W. J.; Laskowski, M. *Biochemistry* **1967**, *6*, 2908–&.

(44) Zhou, C. Z.; Plashkevych, O.; Chattopadhyaya, J. J. *Org. Chem.* **2009**, *74*, 3248–3265.

(45) Fersht, A. *Structure and Mechanism in Protein Science: A Guide to Enzyme Catalysis and Protein Folding*; W. H. Freeman Company: New York, 1998.

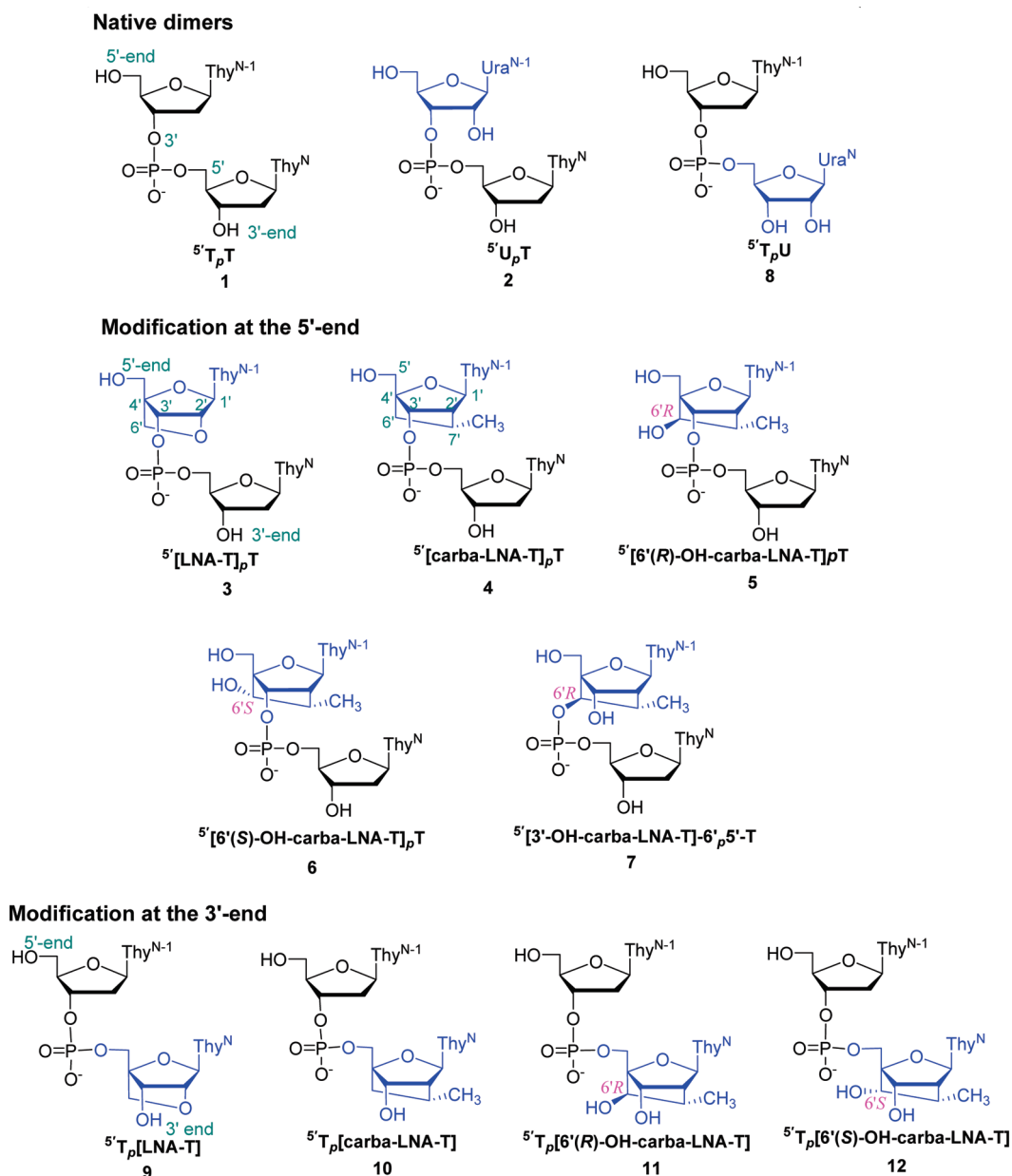


**FIGURE 2.** Structures of the modified dinucleotide models used in this study including native dinucleotides **1**, **2**, and **8**. In the modified dinucleotide models **3**–**7**, the modified nucleosides are located at the 5'-end, whereas in the modified dinucleotide models **9**–**12** the modified nucleosides are located at the 3'-end. All internucleotide linkages (*p*) are 3' → 5' linked except for [3'-OH-carba-LNA-T]-6'<sub>p</sub>5'-T (**7**) which is 6' → 5' linked.

native dimers **1** and **2** is likely to be the result of steric clash and change of hydration (electrostatic) penalty imposed by the 2',4'-locked ring in <sup>5'</sup>[LNA-T]<sub>p</sub>T (**3**). Compared to <sup>5'</sup>[LNA-T]<sub>p</sub>T (**3**), <sup>5'</sup>[carba-LNA-T]<sub>p</sub>T (**4**) has an additional bulky 7'-Me group on the 2',4'-carba-locked ring, which is likely to contribute additional steric clash and alteration of hydration, but it does not seem to be the case because <sup>5'</sup>[carba-LNA-T]<sub>p</sub>T (**4**) exhibits very similar *K<sub>M</sub>* as that of <sup>5'</sup>[LNA-T]<sub>p</sub>T (**3**). Thus, it is likely that the region around C7' (or O2') of N<sup>-1</sup> nucleoside in <sup>5'</sup>[carba-LNA-T]<sub>p</sub>T (**4**) is not involved in any tight interaction with the SVPDE binding site, and instead, steric clash and electrostatics near the C6' of N<sup>-1</sup> nucleoside in <sup>5'</sup>[carba-LNA-T]<sub>p</sub>T (**4**) are apparently more important for retarding SVPDE binding since

<sup>5'</sup>[6'(R)-OH-carba-LNA-T]<sub>p</sub>T (**5**), which has one protruding C6'-OH toward the internucleotide phosphate, shows the largest *K<sub>M</sub>* value, which means a poorer affinity to the enzyme. In contrast, <sup>5'</sup>[6'(S)-OH-carba-LNA-T]<sub>p</sub>T (**6**), in which the 6'(S)-OH group is turning away from the phosphate, has a ca. 2 times larger binding affinity than that of <sup>5'</sup>[6'(R)-OH-carba-LNA-T]<sub>p</sub>T (**5**). The poorer binding affinity of <sup>5'</sup>[6'(R)-OH-carba-LNA-T]<sub>p</sub>T (**5**) can, however, be dramatically improved by 6' → 5'-phosphate linkage in <sup>5'</sup>[3'-OH-carba-LNA-T]-6'<sub>p</sub>5'-T (**7**).

**2.2.2. Different *K<sub>cat</sub>* Modulation by Different 5'-End Modified Dimers.** The decrease of the catalytic efficiency (*K<sub>cat</sub>*) of digestion of **1**–**7** follows this order: <sup>5'</sup>[6'(R)-OH-carba-LNA-T]<sub>p</sub>T (**5**) (302 min<sup>-1</sup>) > <sup>5'</sup>[LNA-T]<sub>p</sub>T (**3**) (237 min<sup>-1</sup>)

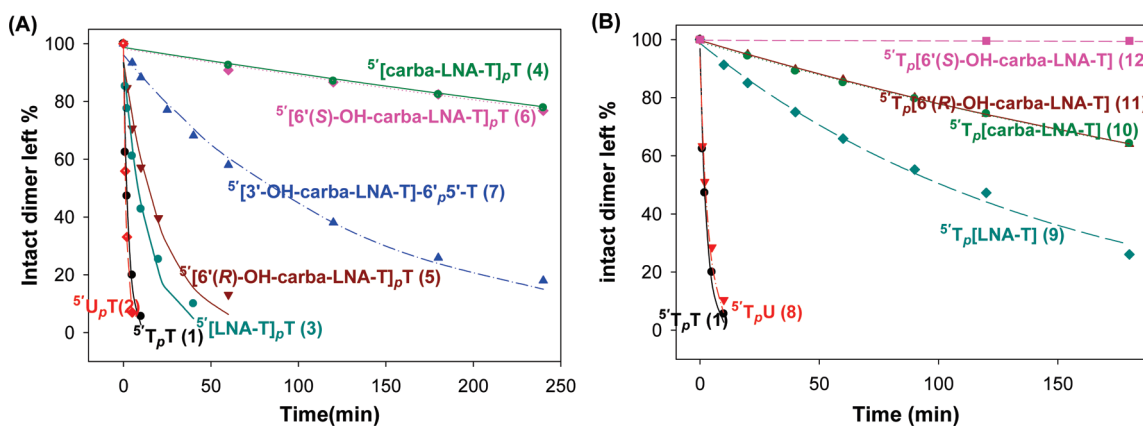


**FIGURE 3.** (A) Comparison of the stabilities of dimers 1–7 upon SVPDE degradation. Digestion curves of 4 (green solid line) and 6 (pink dotted line) overlay each other. (B) Comparison of the stabilities of dimers 9–12 with native dimers 1 and 8 upon SVPDE digestion. Digestion curves of 10 (green dotted line) and 11 (dark red solid line) overlay each other. Note that the differences in the stabilities in the pairs of isomeric 5'-end modified dimers compared to those of respective 3'-end modified dimers is evident from the pairwise comparison of the respective plots in A versus B: 6/12, 5/11, 4/10, 3/9 etc. Digestion conditions: dimer 1 o.d. ( $A_{260\text{ nm}}$ ), 100 mM Tris–HCl (pH 8.0), 100 mM NaCl, 15 mM  $\text{MgCl}_2$ , SVPDE 30  $\mu\text{g}/\text{mL}$ , reaction temperature 21  $^\circ\text{C}$ , total reaction volume 1 mL.

**TABLE 1.** Comparison of Michaelis–Menten Kinetic Parameters<sup>a</sup> of Internucleotidic Phosphate Scission by SVPDE for 3'-Modified and 5'-Modified Dimers with the Native Counterparts

	dimers	$K_M$ ( $\mu\text{M}$ )	$K_{\text{cat}}$ ( $\text{min}^{-1}$ )	$K_{\text{cat}}/K_M$ ( $\mu\text{M min}^{-1}$ )
native dimers	$^5\text{T}_p\text{T}$ (1)	$45.6 \pm 5.6$	$157.5 \pm 5.8$	$3.65 \pm 0.38$
	$^5\text{U}_p\text{T}$ (2)	$14.68 \pm 1.21$	$153.17 \pm 2.50$	$9.74 \pm 0.88$
	$^5\text{T}_p\text{U}$ (8)	$20.0 \pm 1.7$	$114.74 \pm 2.2$	$6.00 \pm 0.06$
5'-modified dimers	$^5\text{[LNA-T]}_p\text{T}$ (3)	$365.5 \pm 44.8$	$236.6 \pm 17.3$	$0.625 \pm 0.037$
	$^5\text{[carba-LNA-T]}_p\text{T}$ (4)	$412.1 \pm 78.4$	$2.21 \pm 0.27$	$0.0059 \pm 0.0003$
	$^5\text{[6'(R)-OH-carba-LNA-T]}_p\text{T}$ (5)	$545.2 \pm 81.9$	$301.9 \pm 29.3$	$0.5865 \pm 0.007$
	$^5\text{[6'(S)-OH-carba-LNA-T]}_p\text{T}$ (6)	$250.2 \pm 21.6$	$1.93 \pm 0.09$	$0.0078 \pm 0.0005$
	$^5\text{[3'-OH-carba-LNA-T]}_p\text{-6}'_p\text{5}'\text{-T}$ (7)	$83.2 \pm 5.6$	$7.57 \pm 0.17$	$0.089 \pm 0.009$
3'-modified dimers	$^5\text{T}_p\text{[LNA-T]}$ (9)	$52.5 \pm 4.4$	$4.0 \pm 0.10$	$0.075 \pm 0.001$
	$^5\text{T}_p\text{[carba-LNA-T]}$ (10)	$313.6 \pm 35.4$	$3.60 \pm 0.23$	$0.011 \pm 0.0007$
	$^5\text{T}_p\text{[6'(R)-OH-carba-LNA-T]}$ (11)	$289.5 \pm 57.1$	$3.60 \pm 0.40$	$0.013 \pm 0.003$
	$^5\text{T}_p\text{[6'(S)-OH-carba-LNA-T]}$ (12)	No cleavage	detected	

<sup>a</sup>All values are averages and standard deviations of three independent experiments.

$> ^5\text{T}_p\text{T}$  (1) ( $157\text{ min}^{-1}$ )  $\approx$   $^5\text{U}_p\text{T}$  (2) ( $153\text{ min}^{-1}$ )  $> ^5\text{[3'-OH-carba-LNA-T]}_p\text{-6}'_p\text{5}'\text{-T}$  (7) ( $7.6\text{ min}^{-1}$ )  $> ^5\text{[carba-LNA-T]}_p\text{T}$  (4) ( $2.2\text{ min}^{-1}$ )  $\approx$   $^5\text{[6'(S)-OH-carba-LNA-T]}_p\text{T}$  (6) ( $1.9\text{ min}^{-1}$ ).  $^5\text{[6'(R)-OH-carba-LNA-T]}_p\text{T}$  (5) exhibits the best catalytic efficiency (despite a very high  $K_M$ ), suggesting the 6'(R)-OH that is directed toward the internucleotidic phosphate plays an important role in assisting scission of the  $P\text{-O}3'$  bond.  $^5\text{[carba-LNA-T]}_p\text{T}$  (4) and  $^5\text{[6'(S)-OH-carba-LNA-T]}_p\text{T}$  (6) exhibit roughly 100 times smaller  $K_{\text{cat}}$  than those of the native 1 and 2.  $^5\text{[3'-OH-carba-LNA-T]}_p\text{-6}'_p\text{5}'\text{-T}$  (7), which contains the 6' $\rightarrow$ 5' phosphate linkage, shows a very small  $K_{\text{cat}}$ , which is slightly higher than those of  $^5\text{[carba-LNA-T]}_p\text{T}$  (4) and  $^5\text{[6'(S)-OH-carba-LNA-T]}_p\text{T}$  (6).

From these kinetics data, we can see that the nuclease resistance of  $^5\text{[LNA-T]}_p\text{T}$  (3) is only slightly improved ( $K_{\text{cat}}/K_M$  difference is around 6 times) compared to that of the native  $^5\text{T}_p\text{T}$  (1), which is mainly attributed to the poorer binding affinity ( $K_M$ ) of the former compared to the that of the latter to the nuclease. Comparison of  $K_M$  and  $K_{\text{cat}}$  for  $^5\text{[LNA-T]}_p\text{T}$  (3) and  $^5\text{[carba-LNA-T]}_p\text{T}$  (4) shows that 100 $\times$  improvement in the nuclease resistance for the latter comes from its much-decreased catalytic efficiency compared to the former, not from the  $K_M$  because it is very comparable for both. Remarkably decreased stability imposed by 6'(R)-OH modification in carba-LNA-T as in  $^5\text{[6'(R)-OH-carba-LNA-T]}_p\text{T}$

(5), as evident from a significant increase of the  $K_{\text{cat}}$  compared to that of  $^5\text{[6'(S)-OH-carba-LNA-T]}_p\text{T}$  (6), is attributed to the fact that the 6'(R)-OH in the former is located on the same side as the internucleotidic phosphate, whereas the 6'(S)-OH in the latter is located on the opposite side of the phosphate. Therefore, the 6'(R)-OH is in steric proximity with the internucleotidic phosphate in the former, is predisposed to H-bonding interaction, and assists in the catalysis.

The observed digestion rates and the  $t_{1/2}$  of the nuclease resistances of dimers 1–7 shown in Figure 3 decreases as the  $K_{\text{cat}}/K_M$  (Table 1) decreases, as expected.

**3.0. Nuclease Resistance of the Internucleotidic Phosphate with 3'-End Modifications at Position "N" in Dimers 9–12.** In order to understand the structure–activity relationship in Michaelis kinetics, we have used isomeric substrates to explore the mode of cleavage of the internucleotidic linkage by SVPDE.

**3.1. Comparison of Relative Nuclease Resistance of Modified Dimers 9–12 with Native 1 and 8.** To compare the relative nuclease resistance of the phosphate with LNA-T or carba-LNA-T modifications at position "N" (at the 3'-end), dimers 8–12 were treated with SVPDE under identical conditions as described in section 2.1. Their nuclease resistances decreases ( $t_{1/2}$ ) in the following order (Figure 3B):  $^5\text{T}_p\text{[6'(S)-OH-carba-LNA-T]}$  (12)  $>$   $^5\text{T}_p\text{[carba-LNA-T]}$

(10) (288 min)  $\approx$   $^5T_p[6'(R)\text{-OH-carba-LNA-T}]$  (11) (277 min)  $>$   $^5T_p[\text{LNA-T}]$  (9) (103 min)  $>$   $^5U_pT$  (8) (2.5 min)  $\approx$   $^5T_pT$  (1) (1.9 min).  $^5T_p[\text{LNA-T}]$  (9) is about 50 times more stable than native  $^5T_pT$  (1).  $^5T_p[\text{carba-LNA-T}]$  (10) and  $^5T_p[6'(R)\text{-OH-carba-LNA-T}]$  (11) have very similar stability, and both of them were only around  $2.5\times$  more stable than  $^5T_p[\text{LNA-T}]$  (9). However,  $^5T_p[6'(S)\text{-OH-carba-LNA-T}]$  (12) with 3'-terminal (i.e., "N") substitution showed unusual nuclease resistance and almost no degradation and could be detected after incubation for 4 h, in contrast with that of the "N<sup>-1</sup>" substituted dinucleotide  $^5[6'(S)\text{-OH-carba-LNA-T}]_pT$  (6), which is degraded  $\sim 20\%$  under identical conditions (compare Figure 3A,B). Finally, this study shows  $^5T_p[6'(S)\text{-OH-carba-LNA-T}]$  (12) has the highest nuclease stability among all 12 dimers studied in this work toward the 3'-exonuclease, which we believe will be useful as take-home lessons for the future design of modifications for therapeutic oligonucleotides.

**3.2. Comparison of Michaelis–Menten Kinetic Parameters of Nuclease Digestion of Modified Dimers 9–12 with Those of the Native 1 and 8.** Subsequently, Michaelis–Menten kinetics of digestions of 3'-end-modified dimers 9–11 by SVPDE were carried out to further explore the mechanism of nuclease resistance of the internucleotidic phosphate with LNA and carba-LNA modifications at position "N".

As shown in Table 1,  $K_M$  of digestion of  $^5T_p[\text{LNA-T}]$  (9) is very similar as that of native counterparts, suggesting that the bulky 2',4'-locked ring in LNA at the 3'-end of the dimer does not impair the binding ( $K_M$ ) of SVPDE. It turns out that it is the reduced catalytic efficiency,  $K_{cat}$ , that leads to its higher nuclease resistance. On the contrary,  $^5T_p[\text{carba-LNA-T}]$  (10) and  $^5T_p[6'(R)\text{-OH-carba-LNA-T}]$  (11) exhibit very similar catalytic efficiency as  $^5T_p[\text{LNA-T}]$  (9) but roughly  $5\times$  higher  $K_M$  values for dimers 10 and 11, suggesting it is the less binding affinities that make dimers with carba-LNA modifications at the 3'-end (residue "N") nucleolytically more stable than their LNA-modified counterpart.

Unlike the 7'-Me modification on the "N<sup>-1</sup>" residue which does not influence  $K_M$ , 7'-Me modification on the "N" residue definitely impairs the binding of SVPDE because  $^5T_p[\text{carba-LNA-T}]$  (10) and  $^5T_p[6'(R)\text{-OH-carba-LNA-T}]$  (11) show nearly  $5\times$  higher  $K_M$  than  $^5T_p[\text{LNA-T}]$  (9). On the other hand, 6'(R)-OH modification on N nucleosides does not seem to influence the SVPDE binding since  $^5T_p[\text{carba-LNA-T}]$  (10) and  $^5T_p[6'(R)\text{-OH-carba-LNA-T}]$  (11) exhibit very similar  $K_M$ .  $^5T_p[6'(S)\text{-OH-carba-LNA-T}]$  (12) is completely resistant to SVPDE digestion, and so the  $K_M$  and  $K_{cat}$  could not be determined. In comparison with  $^5T_p[\text{carba-LNA-T}]$  (10),  $^5T_p[6'(S)\text{-OH-carba-LNA-T}]$  (12) has only one additional C6'(S)-OH protruding toward the internucleotidic phosphate. This C6'(S)-OH could spatially prevent the attacking of SVPDE on the internucleotidic phosphate, and thus, digestion of this phosphate by SVPDE becomes impossible. Hence it seems that bulky (S)-substitution at C6' of carba-LNA could be a very efficient approach to improve the nuclease resistance.

**4.0. Correlation between Catalytic Efficiencies ( $K_{cat}$ ) and Leaving Abilities ( $pK_a$ ) of the Departing 3' (or 6')-OH of LNA or Carba-LNA Derivatives.** During the digestion of 3'-modified dimers 9–11, the leaving native 5'-residues ("N<sup>-1</sup>") were always the T residue (see Figure 2), which results in

similar  $K_{cat}$  in the SVPDE digestion of these dimers. This made us speculate that significantly different  $K_{cat}$ s found in the digestion of 5'-modified dimers 3–7 could be the result of their differently modified departing 5'-nucleoside residues ("N<sup>-1</sup>") with different leaving abilities. Hence, the  $pK_a$ s of the departure 3'(or 6')-OHs of the "N<sup>-1</sup>" nucleosides in 1–7 have been determined by NMR based pH titration experiments.<sup>46,47</sup>

**4.1.  $pK_a$  Values of 3'- and/or 6'-OH of LNA and Carba-LNA Derivatives.** The experimental  $pK_a$  values of the 3'(or 6')-OH of the departing nucleosides 13–18, generated from the SVPDE digestion of dimers 1–7, respectively, decreases in the following order (Figure 4): 6'-OH of 6'(S)-OH-carba-LNA-T (18) ( $pK_a \gg 13.5$ )  $>$  3'-OH of carba-LNA-T (16) ( $pK_a = 13.53 \pm 0.10$ )  $>$  3'-OH of T (13) ( $pK_a = 13.50 \pm 0.19$ )  $>$  3'-OH of 6'(R)-OH-carba-LNA-T (17) ( $pK_a = 13.06 \pm 0.06$ )  $>$  3'-OH of 6'(S)-OH-carba-LNA-T (18) ( $pK_a = 12.91 \pm 0.05$ )  $>$  6'-OH of 6'(R)-OH-carba-LNA-T (17) ( $pK_a = 12.82 \pm 0.03$ )  $>$  3'-OH of U (14) ( $pK_a = 12.62 \pm 0.03$ )  $>$  3'-OH of LNA-T (15) ( $pK_a = 12.10 \pm 0.01$ ). The  $pK_a$  of 3'-OH of LNA-T (15) is even lower than that of U (14), suggesting the constrained conformation of the pentose sugar in LNA-T must play a role in decreasing the  $pK_a$  of 3'-OH. All the nucleosides 15–18 have the same constrained N-type sugar but very different  $pK_a$  values for the 3'-OH, suggesting the  $pK_a$  of 3'-OH can be significantly modulated by modification on the 2',4'-locked ring. This observation is consistent with our previous study that showed the nature of the sugar conformational constrains steer the physicochemical property of nucleoside.<sup>48</sup> The  $pK_a$  modulation in nucleosides 15–18 is likely to be the result of electrostatic effect imposed by the modification. Thus, replacement of electron-withdrawing 2'-O in LNA-T (15) with electron-donating group  $-\text{CH}_2(\text{CH}_3)-$  gives carba-LNA-T (16) whose  $pK_a$  of 3'-OH is 1.4 units larger than LNA-T (15). Further addition of an electron-withdrawing OH group at C6' as in compounds 17 and 18, on the other hand, decreases the  $pK_a$  of 3'-OH. The  $pK_a$  of C6'-OH was remarkably dependent on its orientation: in nucleoside 18, the  $pK_a$  of C6'(S)-OH ( $pK_a \gg 13.5$ ) is much larger than that of the 6'(R)-OH in nucleoside 17. Deprotonation of the 6'(R)-OH in nucleoside 17 could be assisted by the vicinal 3'-OH through formation of intramolecular hydrogen bonding, thus significantly decreasing the  $pK_a$  of the 6'(R)-OH. On the other hand, intramolecular interaction between C6'(S)-OH and 3'-OH in nucleoside 18 is impossible.

**4.2. Correlation between  $\log K_{cat}$  and  $pK_a$  of the Departing 3' (or 6')-OH.** For 5'-end-modified dimers 3–7, the  $\log k_{cat}$  values were almost linearly correlated ( $R = 0.89$ ) to  $pK_a$ s of the departing 3'- or 6'-hydroxyls except that dimer [6'(R)-OH-carba-LNA-T]<sub>p</sub>T (5) escapes the fitting line (Figure 5), thereby suggesting that the SVPDE cleavage mechanism for 5 is different from the rest. The linear correlation of SVPDE cleavage of modified dimers 3, 4, 6, and 7 with those of the  $pK_a$ s of the departing of 3' or 6' oxyanion, however, suggests that the rate-limiting step is the formation of the 3' or 6'

(46) Velikyan, I.; Acharya, S.; Trifonova, A.; Foldesi, A.; Chattopadhyaya, J. J. *Am. Chem. Soc.* **2001**, *123*, 2893–2894.

(47) Acharya, S.; Foldesi, A.; Chattopadhyaya, J. J. *Org. Chem.* **2003**, *68*, 1906–1910.

(48) Plashkevych, O.; Chatterjee, S.; Honcharenko, D.; Pathmasiri, W.; Chattopadhyaya, J. J. *Org. Chem.* **2007**, *72*, 4716–4726.

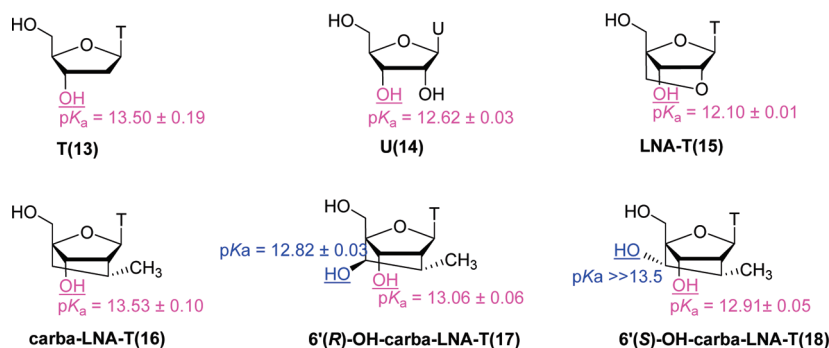


**FIGURE 4.** Structures and  $pK_a$  values of 3'-OH and/or 6'-OH of compounds of 13–18. The  $pK_a$  values were measured by NMR based pH titration experiments.

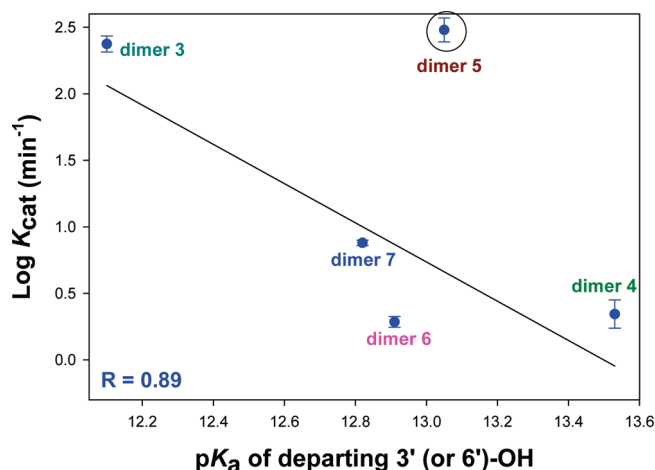


**FIGURE 5.** Correlation between catalytic efficiencies ( $\log K_{cat}$ s from Table 1) and  $pK_a$ s (Figure 4) of the departing 3' (or 6')-OHs for SVPDE mediated digestion of 3–7.  $\log K_{cat}$ s of SVPSDE cleavage of modified dimers 3, 4, 6, and 7 show linear correlation with  $pK_a$ s of the departing 3' or 6' oxyanion, giving Pearson's correlation coefficient  $R = 0.89$ . However, the data for [6'(R)-OH-carba-LNA-T]<sub>p</sub>T (5) do not fit in the correlation plot, thereby suggesting that SVPDE cleavage mechanism for dimer 5 is likely to be different from the rest.

oxyanion. This explains why different leaving group abilities of the 5'-end-modified nucleosides (“N<sup>-1</sup>”) in dimers 3, 4, 6, and 7 lead to their different  $K_{cat}$  values.

For digestion of 3'-modified dimers 9–11, the different  $pK_a$  values of the 3'-OH of the 3'-end-modified nucleosides (“N”) does not result in different  $K_{cat}$  values because the  $pK_a$ s of their 3'-OH have no role to play in the SVDPE enzymatic kinetics since the cleaving 3'O–P bond belongs to the leaving native 5'-residues (“N<sup>-1</sup>”) (see Figure 2).

## Conclusion

This work shows that LNA and carba-LNA modifications at either the “N” or “N<sup>-1</sup>” position can improve the 3'-exonuclease (SVDPE in this study) resistance of internucleolytic phosphate. Michaelis–Menten kinetic studies further demonstrated that when LNA modification is situated at the “N<sup>-1</sup>” position, it increases the nuclease resistance of internucleolytic phosphate mainly by retarding the enzyme binding through steric hindrance and electrostatics. When carba-LNA modification occurs at the “N<sup>-1</sup>” position of the dimer, it exerts a similar magnitude of steric hindrance for

binding to the enzyme, but the catalytic efficiency ( $K_{cat}$ ) of degradation of the internucleolytic phosphate is 100 times smaller compared to that of the LNA-modified counterpart. We found that for the digestion of dimers with LNA or carba-LNA modification at “N<sup>-1</sup>” position by SVPDE, departure of 3'-O<sup>-</sup> is the rate-limiting step and the  $pK_a$  of 3'-OH of carba-LNA is 1.4 units higher than that of LNA. Hence, it is the more basic property of 3'-OH of carba-LNA-T that makes it a less labile leaving group during 3'-exonuclease-mediated degradation than that of LNA; thus, a much lower  $K_{cat}$  is observed for digestion of carba-LNA relative to digestion of LNA.

When LNA or carba-LNA modification is located at the 3'-terminus (position “N”), LNA improves the exonuclease resistance by decreasing the  $K_{cat}$ . Carba-LNA modification exhibits higher nuclease resistance than LNA, which is mainly because the carba-LNA-T-modified nucleoside has less binding affinity toward 3'-exonuclease.

C6'-OH substitution on carba-LNA can modulate the 3'-exonuclease activity to a different degree depending upon the chirality of the C6'-OH as well as the modification position (“N” or “N<sup>-1</sup>”) in the dimer. Thus, the C6'(S)-OH substitution at the 5'-end (“N<sup>-1</sup>”) in <sup>5</sup>[6'(S)-OH-carba-LNA-T]<sub>p</sub>T (6) does not change the 3'-exonuclease resistance for the internucleolytic phosphate (compared to that of <sup>5</sup>[carba-LNA-T]<sub>p</sub>T (4) because the C6'(S)-OH has an opposite orientation (and further away) with respect to the phosphate. In contrast, C6'(R)-OH substitution at the 5'-end (“N<sup>-1</sup>”) in <sup>5</sup>[6'(R)-OH-carba-LNA-T]<sub>p</sub>T (5) considerably enhances the 3'-exonuclease activity for the internucleolytic phosphate (compared to that of <sup>5</sup>[carba-LNA-T]<sub>p</sub>T, 4) because its C6'(R)-OH has the same orientation (and is nearer) with respect to the phosphate. *On the contrary, C6'(S)-OH substituted or C6'(R)-OH substituted carba-LNA modification at the 3'-end (“N”) has a completely opposite effect:* When the C6'(S)-OH analogue is located at the 3'-end (“N”) in <sup>5</sup>T<sub>p</sub>[6'(S)-OH-carba-LNA-T]<sub>p</sub> (12), it is completely resistant to 3'-exonuclease because the C6'(S)-OH protrudes toward the phosphate, probably retarding the attacking of SVPDE on the phosphate. In contrast, C6'(R)-OH substitution at the 3'-end (“N”) in <sup>5</sup>T<sub>p</sub>[6'(R)-OH-carba-LNA-T]<sub>p</sub> (11) exerts *no* influence on degradation of internucleolytic phosphate (compared to that of <sup>5</sup>T<sub>p</sub>[carba-LNA-T]<sub>p</sub> (10) because its C6'(R)-OH has an opposite orientation (and further away) with respect to the phosphate.

## Implications

This study has deep implications for our understanding of design principles of new nuclease resistance oligonucleotides for therapeutic application. For example, the chiral discrimination of the hydroxyl group at C6' of carba-LNAs to engineer their nuclease stability can further be extended through the synthesis of 6'-monoalkyl (pure *S* and *R* at C6') diastereomeric carba-LNAs or 6'-dialkyl (ethyl, propyl, butyl, or homologues) carba-LNAs because (1) the 6'-alkyl group(s) will exert strong steric hindrance for 3'-exonuclease and thus decrease binding affinity greatly toward nuclease when this modification is located at the N<sup>-1</sup> position; (2) just like the 6'(S)-OH in T<sub>p</sub>[6'(S)-OH-carba-LNA-T] (**12**), 6'-alkyl group(s) when substituted in carba-LNA at "N" position in the modified oligos will retard nucleophilic cleavage of the internucleotidic phosphate by 3'-exonuclease; and (3) the electron-donating properties of alkyl groups at C6' will make the 3'-OH much less acidic, thereby decreasing the catalytic efficiency (*K*<sub>cat</sub>) of scission of internucleotidic phosphate when this modification is located at the N<sup>-1</sup> position. Synthesis of these molecules and their nuclease resistance properties are in progress in our laboratory. It should be noted that synthesis of C6'(S or R)-ethyl-LNA has been reported by Seth et al. very recently,<sup>49</sup> and oligonucleotides with these modifications have been found to indeed show striking affinity toward target RNA as well as unusual nuclease resistance.

## Experimental Section

**Materials.** Phosphodiesterase I from *C. adamanteus* (E. C.3.1.4.1, SVPDE) was obtained from a commercial supplier. This enzyme was obtained as a powder, and after reception, 1.82 mg (100 unit) of this enzyme was resuspended at a concentration of 1 mg/mL in 110 mM Tris-HCl, pH 8.0, 110 mM NaCl, 15 mM MgCl<sub>2</sub>, and 50% glycerol. This enzyme solution was kept at -20 °C for digestion study. Under this storage condition, we did not observe obvious activity variation for at least 6 months.

Dimer nucleotides **1–6** and **8–12** were synthesized using an automated DNA/RNA synthesizer (ABI 394 model) based on phosphoramidite chemistry according to previously reported procedures.<sup>30,50,51</sup> For synthesis of dimers **9–12**, universal support II (purchased from a commercial supplier) was used, and the cleavage was carried out according to the product description. The dimer nucleotides **7** were obtained by hydrolysis of D<sub>2</sub>-CNA.<sup>44</sup> After synthesis and deprotection, the obtained crude dimers were purified by preparative reversed-phase (RP) HPLC: Kromasil 100, C18, 5 μm, 250 × 8 mm; 0 → 10 ft → 30 ft, A → A/B = 1/9 → A/B = 5/5, v/v with a flow 1.2 mL/min at room temperature. UV detector with detecting wavelength of 260 nm was used. HPLC buffer A: 0.1 M TEAA in H<sub>2</sub>O-CH<sub>3</sub>CN (95/5). HPLC buffer B: 0.1 M TEAA in H<sub>2</sub>O-CH<sub>3</sub>CN (50/50). The integration of the dimers **1–12** was verified by MALDI-TOF mass spectroscopy: **1**, [M + H]<sup>+</sup> found 546.5, calcd 547.1; **2**, [M + H]<sup>+</sup> found 548.5, calcd 549.1; **3**, [M + H]<sup>+</sup> found 574.2, calcd 575.1; **4**, [M + H]<sup>+</sup> found 586.3, calcd 587.1; **5**, [M + H]<sup>+</sup> found 602.7, calcd 603.0; **6**, [M + H]<sup>+</sup> found 602.7, calcd 603.0;

**7**, [M + H]<sup>+</sup> found 603.0, calcd 603.0; **8**, [M + H]<sup>+</sup> found 548.2, calcd 549.1; **9**, [M + H]<sup>+</sup> found 574.4, calcd 575.1; **10**, [M + H]<sup>+</sup> found 586.3, calcd 587.1; **11**, [M + H]<sup>+</sup> found 602.5, calcd 603.0; **12**, [M + H]<sup>+</sup> found 602.4, calcd 603.0.

**Relative Stabilities of Dimers 1–12 upon SVPDE Degradation.** A 1 o.d. (*A*<sub>260 nm</sub>) dimer and 30 μL (1.65 unit) of SVPDE solution was mixed in 1 mL of buffer containing 100 mM Tris-HCl, pH 8.0, 100 mM NaCl, and 15 mM MgCl<sub>2</sub>. This mixture was kept at 21 °C, and aliquots (100 μL) were taken at proper time points and quenched with 100 μL of 10 mM EDTA solution followed by freezing with anhydrous ice quickly. Then the aliquots were analyzed by analytical RP-HPLC: Kromasil 100, C18, 5 μm, 100 × 4.6 mm; 0 → 10 ft → 20 ft, A → A/B = 1/9 → A/B = 38/62, v/v. Flow of 1 mL/min at room temperature was used in a UV detector with detecting wavelength of 260 nm. The total percentage of integrated dimers was plotted against time points to give the degradation curves (Figure 3), and the pseudo-first-order reaction rates (*k*<sub>obs</sub>) could be obtained by fitting the curves to single-exponential decay functions. *t*<sub>1/2</sub> was calculated according to this equation: *t*<sub>1/2</sub> = ln 2/*k*<sub>obs</sub>.

**Michaelis–Menten Kinetics of SVPDE Digestion.** Dimer (concentration varied from 23.8 to 416.6 μM) and SVPDE (for different dimers, different concentrations of SVPDE were used: dimers **1** and **8**, 0.022 unit; dimer **2**, 0.017 unit; dimers **3** and **5**, 0.083 unit; dimers **7** and **9**, 0.55 unit; dimers **4**, **6**, **10** and **11**, 1.1 unit) were mixed in 500 μL of buffer containing 100 mM Tris-HCl, pH 8.0, 100 mM NaCl, and 15 mM MgCl<sub>2</sub> at 21 °C. Aliquots were taken at proper time points (less than 6% digestion occurred) and quenched with EDTA solution followed by freezing with anhydrous ice. The aliquots were then analyzed by analytical RP-HPLC as described above. The total percentage of integrated dimers was plotted against time points to give the initial velocities (*v*<sub>0</sub>) of the reactions (see the Supporting Information). Values of the kinetic parameters (*K*<sub>M</sub> and *V*<sub>max</sub>) in this method were determined directly from *v*<sub>0</sub> versus concentration of substrate ([S]) plots (see the Supporting Information) using a correlation program where the correlation equation was *y* = *ax*/(*b* + *x*), where *a* = *V*<sub>max</sub> and *b* = *K*<sub>M</sub>. *K*<sub>cat</sub> was obtained from this equation: *K*<sub>cat</sub> = *V*<sub>max</sub>/*E*<sub>0</sub>, where *E*<sub>0</sub> corresponds to the concentration of enzyme used in the reaction. All values are averages with standard deviations of three independent experiments.

**pH-Dependent <sup>1</sup>H NMR Measurement and Experimental p*K*<sub>a</sub> Determination.** All NMR experiments were performed using Bruker DRX-600 spectrometers. The 2.5 mM NMR samples of compounds **13–18** were prepared in D<sub>2</sub>O solution with δ<sub>DSS</sub> = 0.015 ppm as internal standard. All pH-dependent NMR measurements have been performed at 298 K. The pH values (with the correction of deuterium effect) correspond to the reading on a pH meter equipped with a calomel microelectrode (in order to measure the pH inside the NMR tube) calibrated with standard buffer solutions (in H<sub>2</sub>O) of pH 7, 10, and 12.45. The pD of the sample has been adjusted by simple addition of microliter volumes of NaOD solutions (1, 0.5, and 0.1 M). The pH values are obtained by the subtraction of 0.4 from corresponding pD values [pH = pD - 0.4]. All <sup>1</sup>H spectra have been recorded using 128 K data points and 64 scans.

The pH titration studies were done over a range of pH (9 < pD < 13.5) with (0.1–0.3) pH interval. The pH-dependent <sup>1</sup>H chemical shifts (δ, with error ± 0.001 ppm) of H3' (or H2' if determination of chemical shift of H3' is difficult because of overlay) and H6' for all compounds have shown a sigmoidal behavior (see the Supporting Information), which corresponds to 3'-OH or 6'-OH deprotonation. Values of the p*K*<sub>a</sub>s have been determined by fitting the titration curves employed with a Hill coefficient set close to unity. The pH-dependent <sup>1</sup>H chemical shifts of H6' of 6'(S)-OH-carba-LNA-T(**18**) do not change with pH up to 13.5; hence, the p*K*<sub>a</sub> of the 6'(S)-OH in

(49) Seth, P. P.; Vasquez, G.; Allerson, C. A.; Berdeja, A.; Gaus, H.; Kinberger, G. A.; Prakash, T. P.; Migawa, M. T.; Bhat, B.; Swayze, E. E. *J. Org. Chem.* **2010**, *75*, 1569–1581.

(50) Zhou, C. H.; Honcharenko, D.; Chattopadhyaya, J. *Org. Biomol. Chem.* **2007**, *5*, 333–343.

(51) Zhou, C. Z.; Pathmasiri, W.; Honcharenko, D.; Chatterjee, S.; Barman, J.; Chattopadhyaya, J. *Can. J. Chem.* **2007**, *85*, 293–301.

6'(S)-OH-carba-LNA-T (**18**) must be much higher than 13.5. The  $pK_a$  of 2'-OH ( $pK_a = 12.62 \pm 0.03$ ) of uridine (**14**) has been measured previously in this way by us.<sup>46</sup> Since the adjacent 2'-OH and 3'-OH can interact during deprotonation, the obtained  $pK_a$  value is supposed to be the combined effect of 2'-OH and 3'-OH.<sup>52</sup> Some other experiments also support the conclusion that 2'-OH and 3'-OH in ribonucleoside have similar  $pK_a$  values.<sup>53</sup> Hence, we define the  $pK_a$  of 3'-OH of uridine to be 12.62.

(52) Izatt, R. M.; Hansen, L. D.; Rytting, J. H.; Christen, J. *J. Am. Chem. Soc.* **1965**, *87*, 2760–2761.

(53) Wolfenden, R.; Rammler, D. H.; Lipmann, F. *Biochemistry* **1964**, *3*, 329–338.

**Acknowledgment.** Generous financial support from the Swedish Natural Science Research Council (Vetenskapsrådet), the Swedish Foundation for Strategic Research (Stiftelsen för Strategisk Forskning), and the EU-FP6 funded RIGHT project (Project no. LSHB-CT-2004-005276) is gratefully acknowledged.

**Supporting Information Available:** NMR data of compounds **13–18**, HPLC profiles of SVPDE digestion, kinetics plots of SVPDE digestion, and pH titration plots. This material is available free of charge via the Internet at <http://pubs.acs.org>.